Revista Brasileira de Aplicações de Vácuo, v. 27, n. 2, 97-102, 2008.

PHYSICAL PROPERTIES OF (Al-Si-Cu)-N THIN FILMS DEPOSITED BY DC-REACTIVE MAGNETRON SPUTTERING

R. Figueroa[1*]; I. Doi[1,2]; J.A. Diniz[1,2]
[1] *UNICAMP, Center for Semiconductor Components, 13.083-870 Campinas, SP, Brazil*
[2] *UNICAMP, School of Electrical and Computer Engineering, 13.083-970 Campinas, SP, Brazil*

Received: March 26, 2008; Revised: June 29, 2008

Keywords: (Al-Si-Cu)-N, sputtering, dielectric films, morphology, optical properties.

ABSTRACT

In this work, the properties of (Al-Si-Cu)-N thin films prepared by D.C. Reactive Magnetron Sputtering were studied using different characterization techniques. The electrical properties of the obtained samples show that they are promising material in regard to the applications in microelectronics devices. The high resistivity and FTIR characteristics observed in the analyzed samples, indicate that the films are mostly consisted of Al-N bonds and that they are a prospective dielectric material.

1. INTRODUCTION

AlN thin films have been considered of great interest at various applications, such as piezoelectric material for high frequency integrated circuit devices such as surface acoustic wave (SAW) and film bulk acoustic resonators (FBARs) [1-3]. AlN also has attractive applications at photonic and photo-emitting devices. Nano-scale properties at the surface enable the films to exhibit photonics features [4]. AlN thin films can be prepared by several and different techniques including Chemical Vapor Deposition – CVD [5,6], arc plasma [7], and sputtering [8-10]. Among the mentioned techniques, sputtering deposition is the preferred technique to prepare polycrystalline AlN thin films on larger substrates, due to the better c-axis growth enhancing the piezoelectric performance in the films mentioned. In the present work, we report results of the physical properties of the (Al-Si-Cu)-N thin films, deposited by DC-reactive magnetron sputtering, to explore this material at different applications for FBARs, SAW, optical and electronic devices. Initially, we reported the compositional analysis, at function of nitrogen fluxes, on deposited samples. Next of this, we show the relationship between the physical properties of thin films with the sputtering deposition parameters, such as, deposition power and reactive-gas flux, on deposited samples. We also have evaluated how the optical and morphological properties of these films influences the energy and shape of infrared absorption bands of polycrystalline (Al-Si-Cu)-N thin films. Next, we present electrical characteristics of films showing a metallic and semiconductor state depending of the deposition parameters. Additionally, surface and cross section images from samples were acquired to characteristic morphological and colunar structure of the thin films. Finally, Roughness analysis of the films was studied in function of the deposition power.

2. EXPERIMENTAL PROCESS

The (Al-Si-Cu)-N thin films were prepared on p-type Si (100) substrates in an argon (Ar) and nitrogen (N_2) gas atmosphere using a d.c. reactive magnetron sputtering system, ULVAC MCH 9000. Silicon (20~25 Ω·cm) wafers were cleaned by standard RCA cleaning process and the used magnetron sputtering source has a composite AlSiCu (98.5%/1%/0.5%) target of 10-in. diameter and it was placed parallel to the substrate. Distance between them was 55 mm. Prior to (Al-Si-Cu)-N film deposition, the sputtering chamber was evacuated to a pressure below 4.0×10^{-5} Pa and then high purity Ar (50 sccm) and N_2 gas were introduced through independent mass flow controller in three deposition series (table 1). As the substrate was not heated, the substrate temperature increase was only dependent on self-heating due to d.c. plasma. The chemical composition of the thin films was determined by a LV-SEM JSM 5900LV equipped with an electron dispersive x- ray (EDS, Noran Voyager). The energy of the incident electrons was 25 kV and the exposition time was usually 30 seconds. The films thickness was measured with a Dektak 6M stylus profilometer and the chemical bonds of the obtained samples from several spectra determined by Fourier transform infrared spectroscopy (FTIR), which were carried out with a Digilab System, in the wavelength range from 400 to 3500 cm^{-1} with the resolution of 4 cm^{-1}. The measurements were performed using oblique incidence, which means that the electric field was not necessarily parallel to the sample surface.

Table 1 - Sputtering conditions of (Al-Si-Cu)-N films

Deposition series	1	2	3
Power (KW)	0.5 – 4.5	1.0 – 5	3
Flux (sccm)	Ar: 50 N_2: 75	Ar: 50 N_2: 260	Ar: 50 N_2: 10-100

The ellipsometry measurements of (Al-Si-Cu)-N films were carried out at room temperature, in the wavelength of 632.8

* robinsonfc@ccs.unicamp.br

nm with a Rudolph/Auto EL 33.2.4C. Based on the obtained ellipsometry data, the refraction index “n” of the produced samples was determined using one-layer model. Electrical measuring was realized with four point method. The surface and cross sectional morphologies of obtained (Al-Si-Cu)-N films, analyzed by scanning electron microscopy using a FEG-SEM JSM 6330F. The surface roughness of some samples were obtained with an atomic force microscopy (AFM) (DI Nanoscope IIIa) operated in the tapping mode in ambient conditions.

3. RESULTS AND DISCUSSION

3.1. Compositional Analysis

Fig. 1 shows the EDS results for the (Al-Si-Cu)-N thin films deposited at differents power (series 1). Aluminium and nitrogen composition increases on the thin films with the deposition power. Moreover, the graphic reveals the effect of deposition power at the nitrogen composition increasing on the thin film, even though N_2 flux was kept constant at 75 sccm. This observation was assumed as the influence of the adatom energy descomponing gas phase of N_2. Consequently, the nitrogen concentration increases with the adatom energy atomic. Fig. 2 (Al-Si-Cu)-N presents the thin films composition as a function of N_2 flow (deposition series 3). At lower fluxes of 40sccm, nitrogen composition continously increases with the nitrogen flux. Different behavior is observed for the aluminum composition, which shows the instability, first increasing to a high level and then decreasing to a minimum level at the N_2 flow of 20 sccm and 50 sccm, respectively. In this range, the films also are metallic. For higher fluxes above 40 sccm, the compositional behavior is more stable for both N and Al. It is observed that in this range of nitrogem flow, the nitrogem composition is higher than that of aluminum. In this conditions its knowed that AlN thin films showing semiconductor properties. Copper element was not founded in this experiment, and Silicon composition are not showed because our results involve mixture Silicon from thin film and substrate.

3.2. Deposition rate

Fig. 3 shows the dependence of the deposition rate of (Al-Si-Cu)-N films, sputtered at several deposition power values (series 1 and 2). For all produced thin films, the deposition rate increases with the increase of applied power. For each series 1 and 2, such increasing of the deposition rate on the samples can be attributed to the increasing in the sputtering efficiency with the deposition power [11-13]. Furthermore, when the used deposition power is increased to the values higher than 2 KW, and at lower nitrogen flow (from series 1 and series 2), the deposition rate becomes higher in comparison to the samples obtained with high nitrogen flows (series 2). It means that at lower flows of reactive gas, the mean free path of the sputtered atoms is higher leading to a rapid deposition of the films. At applied power lower than 2 KW, the observed deposition rate is low and similar for both cases of nitrogen flows (75 and 260 sccm). In these power conditions, the deposition rate keeps almost constant as the sputtered atoms rate is low enough. Fig. 4 shows the evolution of deposition rate under various nitrogen flow conditions, at deposition power of 3 KW (series 3). The deposition rate decreases with the increasing of the nitrogen flows. However, two linear decreasing behaviors can be observed. Firstly, a rapid decreasing with the nitrogen flows occurs between 10 – 40 sccm, showing the deposition rate high sensitivity with nitrogen flow variations. Moreover, the samples deposited in this nitrogen flow range exhibited a metallic surface appearance. At nitrogen flows higher than 40 sccm, the deposition rate shows a slow linear behavior to the reactive gas. Probably at higher nitrogen flows such as 40 sccm, the argon ionization rate becomes controlled by reactive gas pressure decreasing the sputtering efficiency. In regard to the reproducibility of the deposited films, the results show that better stable deposition conditions for obtaining the (Al-Si-Cu)-N films are with nitrogen flows higher than 40 sccm.

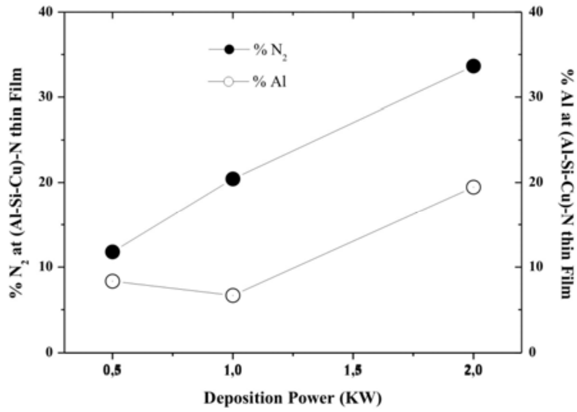

Figure 1 - Compositional behavior of elements deposited at different deposition power. Both Ar and N_2 fluxes were 50 sccm and 75 sccm, respectively.

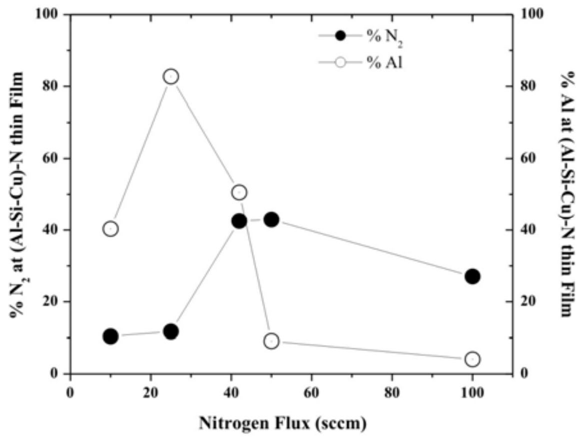

Figure 2 - Composition of elements present on the (Al-Si-Cu)-N thin films. Deposition power and Argon flux were 3 KW and 50 sccm, respectively.

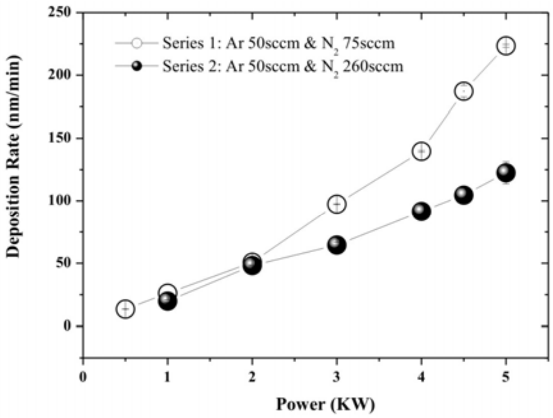

Figure 3 - Deposition rate of the (Al-Si-Cu)-N films at different power and at two nitrogen flow series. All films were deposited at 50 sccm Argon flow. In both series of samples, the influence of the power on deposition rate is observed, being more enhanced at lower nitrogen flows (75 sccm).

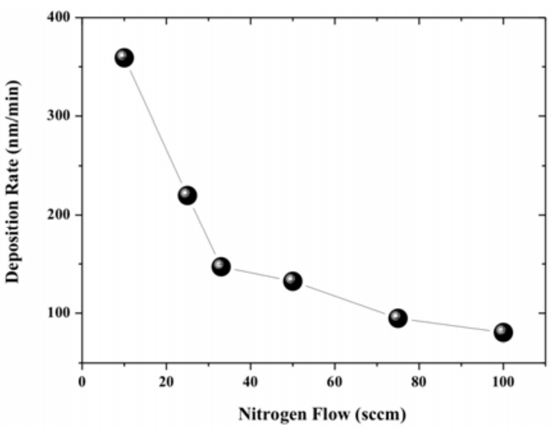

Figure 4 - Deposition rate of the (Al-Si-Cu)-N films at different nitrogen flows. All films were deposited at 50 sccm Argon flow and at deposition power of 3 KW. Deflection point occurs at 40 sccm of N_2 flow and it shows two linear behavior of deposition rate, being the stable region between 40 – 100 sccm.

3.3. Optical Properties

Fig. 5 shows FTIR spectra of the films deposited at different powers using argon flows of 50 sccm and 75 sccm of nitrogen (series 1). At lower sputtering power the obtained (Al-Si-Cu)-N films, not exhibited a well defined absorption peaks. The two peaks, one at wavelength approximately 678 cm^{-1} and another at approximately 605 cm^{-1}, can be attributed to E1(TO) and A1(TO) modes of wurtzite AlN[14,15]. Same behavior was observed at the series 2 too. In both series (1 and 2), a strong absorption peak appears with the increase of deposition power. Moreover, a split peak profiles were found for the upper power of 2 KW. For samples of the series 2, two overlapping peaks were decomposed from the measured absorption spectra, assuming peak profiles as Lorentzian distribution to obtain their peak energy and integrated area. At high powers the films showed a more intense E1(TO) absorption peaks in relation to A1(TO). This effect on material bonding can be evaluated from their respective peaks area (a(E1) and a(A1)). Fig. 6 illustrates the variation behavior of the absorption peak area for the fabricated samples and its correlation with the deposition power. The deposition conditions of the analyzed samples were in accordance with the series 2. However, for both cases (series 1 and 2), the absorption peak at 678 cm^{-1} increases more than that of the wavelength of 605 cm^{-1}. But for the samples prepared at lower nitrogen flows (series 1), the relation a(E1)/a(A1) is higher than those observed for the films deposited at high nitrogen flows, indicating presence of more numbers of wurtzite modes at lower nitrogen flows.

Fig. 7 shows FTIR absorption spectra of the films deposited with different flow rates Ar/N_2 (samples of the series 3). FTIR peak was not observed in the film deposited under lower nitrogen flows. With increase of the nitrogen flow, higher than 42 sccm, the two peaks E1(TO) and A1(TO) appear . No significant Si-Cu, Al-Si, and Al-Cu components influence was found on the absorption bond of all films. Probably, because of little composition of sputtered-material in the target, such as Si(1%) and Cu(0.5%).

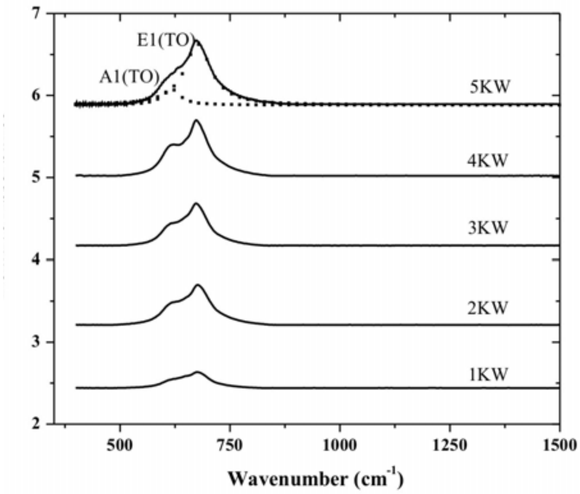

Figure 5 - FTIR spectra of (Al-Si-Cu)-N films deposited under different power. The results show more defining absorption peaks in samples deposited at higher deposition powers.

3.4. Electrical Resistivity

The electrical resistivity of all samples was measured by the four-point probe method. Fig. 8 shows the resistivity behavior of the samples as a function of the used nitrogen flows in their preparations. The transition from electrically conductive to fully insulating films is clearly observed for the series of the samples deposited at 75 sccm of nitrogen (series 1). For the case of films deposited at 260 sccm of nitrogen (series 2), the measurements of the samples resistivity was not able to obtain, as their values were higher than the upper limit of the four-point equipment. The observed results indicate a high insulating properties of the produced films.

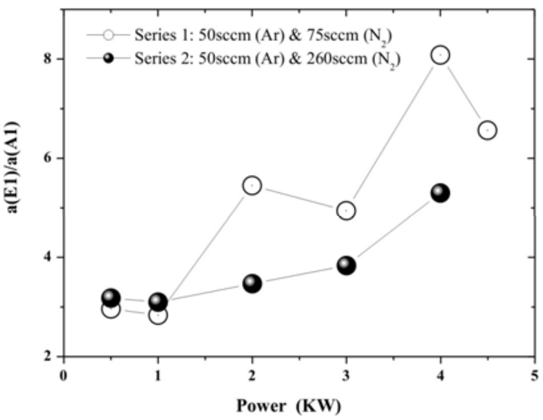

Figure 6 - Relationship between IR vibrational properties of (Al-Si-Cu)-N films and deposition power for the samples obtained using two different nitrogen flows. a(E1)/a(A1) represents the ratio of integrated areas of the E1(TO) and A1(TO), respectively.

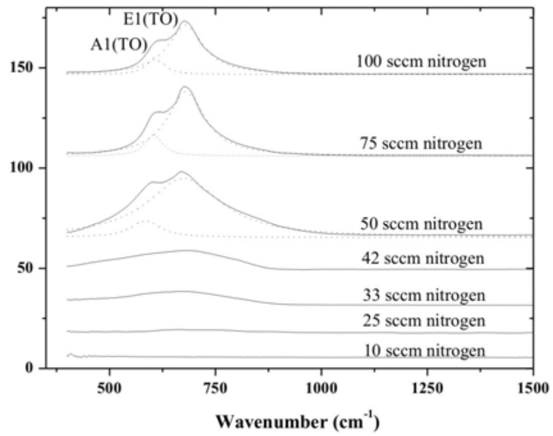

Figure 7 - FTIR spectra measured in (Al-Si-Cu)-N thin films deposited in different nitrogen flows. Deposition power 3 KW, and Argon flow rate 50 sccm. At higher flows of N_2 (>50 sccm), dashed curves show Lorentzian best-fit to the two experimental peaks at 605 and 678 cm^{-1}, corresponding to A1(TO) and E1(TO) absorption bands, respectively.

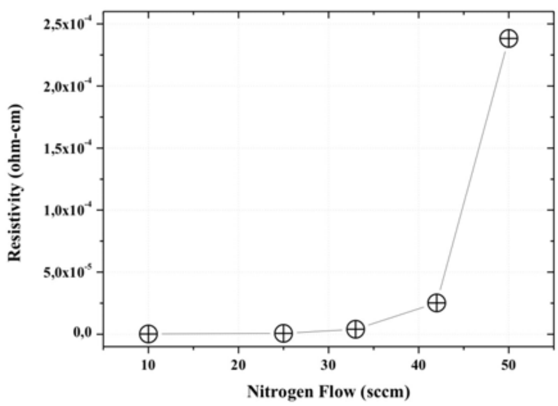

Figure 8 - Electrical resistivity measured in the samples deposited at different flows of nitrogen. Deposition power of 3 KW and Argon flow of 50 sccm. For higher nitrogen flow (40 sccm) its worth to note that the resistivity behavior exhibit an abrupt increase in their values.

3.5. Refraction Index

Fig. 9 shows the refraction index of the thin films deposited with different powers according to series 1. Refraction index have a rapid increasing with the deposition power in the range of a dielectric material between 2.0-2.7. Since the refraction index is related to film density [16], as well as its composition, one can consider as the best choice the range between 0.5 – 4.0 KW as a suitable deposition power. This deposition parameter has a thorough influence on the film density. Samples of the series 2 were not analyzed, since N2 fluxes of this series are excessively higher than fluxes of the series 1.

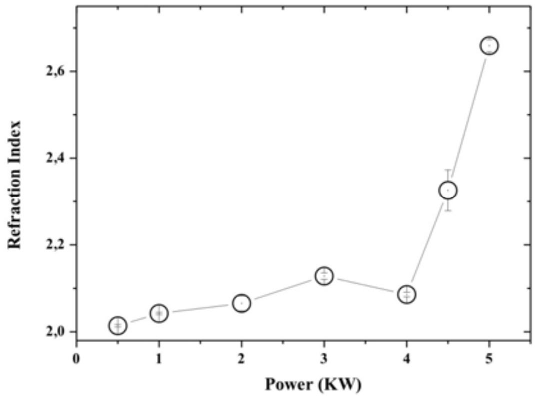

Figure 9 - Influence of the deposition power on the refraction index of (Al-Si-Cu)-N. Ar at 50 sccm and N_2 at 75 sccm. Samples with better stable refraction index are found at deposition powers between 1-4KW.

Fig. 10 shows the effect of N_2 reactive gas flow on the refraction index of (Al-Si-Cu)-N films deposited at 3 KW power (series 3). As the figure shows, between 1.2 – 2.2, the refraction index changes abruptly at nitrogen flow of 40 sccm. This change can be attributed to transition of a material metallic to dielectric material.

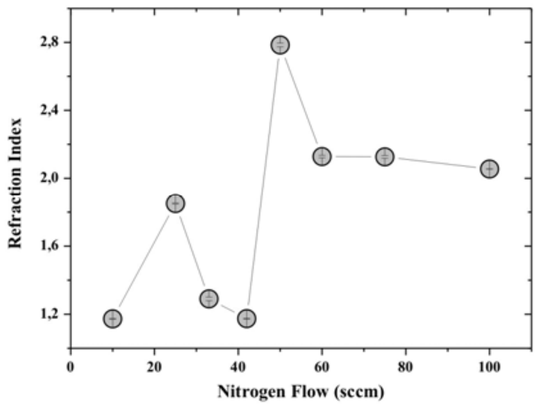

Figure 10 - Influence of the nitrogen flux on the refraction index of (Al-Si-Cu)-N films. Deposition power was applied at 3.0 KW. The curve shows two ranges of refraction index values for two ranges of nitrogen flows. For nitrogen flows between 10-40 sccm, thin film samples showed a metallic surface. For higher nitrogen flows to 40 sccm, the samples showed a blue color surface.

3.6. Morphology of the films

Some morphology of the deposited films is shown in Fig. 11. Once can use the SEM-FEG images and the deposition rate of each sample, in order to obtain an empirical relationship between grain size, mean free path, power, and flows. When the power increases from 1 KW to 5 KW, at 260 sccm N_2 flow and kept constant the Ar flow at 50 sccm (series 2), the grain size increases from 18.6 ± 2.4 to 43.7 nm ± 5.6 nm. Whereas when the deposition power increases from 1 to 4.5 KW, at 75 sccm N_2 flow and 50 sccm Ar flow (series 1), the grain size increases from 14.8 ± 2.4 to 58.9 nm ± 3.4 nm. Considering both series (1 and 2), when the N_2 flow increases the surfaces of the films becomes rougher and with larger grain size, Fig. 11(a, c). Such morphological behavior, at increasing nitrogen flows, is caused by the reduction of mean free path of sputtered atoms that will impinge over the film surface during the deposition. On the other hands, in the films produced at higher deposition powers, we observe that grain size increases with the nitrogen flow diminishing Fig. 11(b, d). This effect of increasing on the grain size may be caused by the decreasing number of collisions of the sputtered atoms, in the plasma, with the decreasing of the reactive gas [17]. In addition, Fig 12 shows a SEM-FEG image of the cross sectional structure of the (Al-SI-Cu)-N film deposited at 4 KW. Argon and N_2 flows were kept at 50 sccm and 75 sccm, respectively. From the initial stages of the deposition process, a randomly oriented columnar structure is evident within the (Al-Si-Cu)-N film. Over the structural part, the film exhibits uniformly columnar type of structure. The columns width is about 40 mn. This result has direct relation with the morphological grain size of thin films. Finally, Fig. 13 shows the surface roughness behavior of the films deposited of accord to the series 1, from AFM data at different scan size. The AFM measurements showed that the surface roughness (RMS) of the films from series 1 vary from 0.5 to 1.1 nm at the power range 0,5-5KW. As expected, roughness of the films increases with the increases the deposition power. With this in mind and considering the grain size as a direct function of deposition power, that was observed from the SEM/FEG results, we can assume that during deposition, adatomic bias event was lower if we consider the roughness scale de our results.

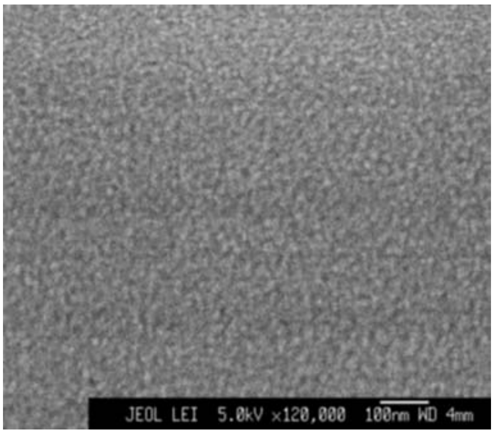

(a)

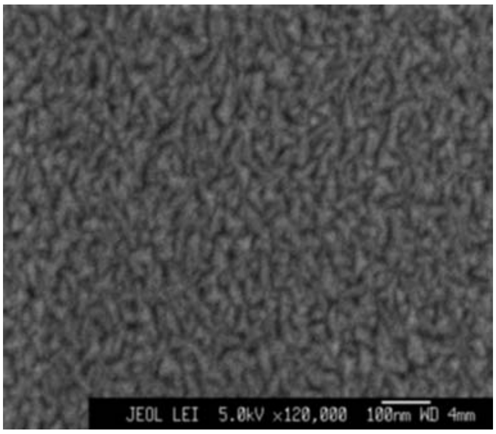

(b)

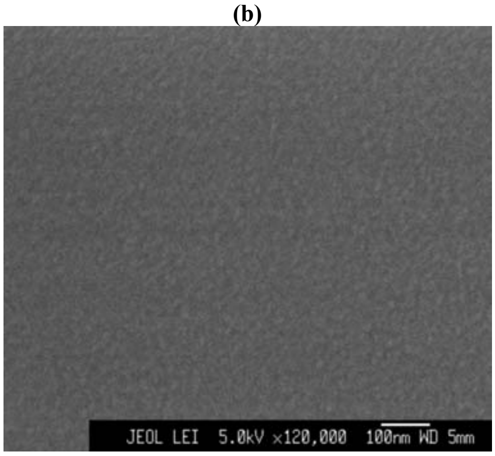

(c)

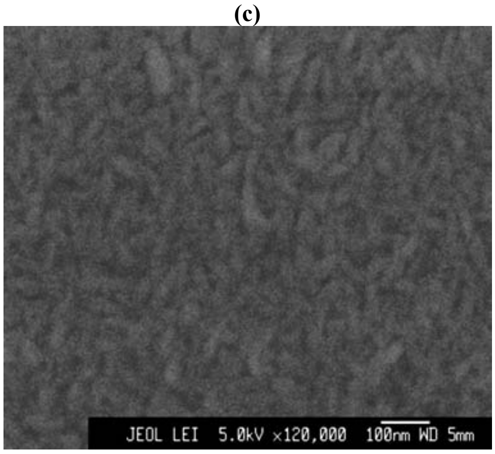

(d)

Figure 11 - SEM-FEG micrographs of the surface morphology of (Al-Si-Cu)-N films deposited at two flow series and at two power (a) 50 sccm Ar, 260 sccm N_2, 1KW (b) 50 sccm Ar, 260 sccm N_2, 5KW (c) 50 sccm Ar, 75N_2, 1KW (d) 50 sccm Ar 75 N_2, 4.5 KW. In cases with higher deposition power, the surface of the films was covered with abnormally grown large elongated grain. When the N_2 flow increases, the surfaces of the films becomes rougher.

4. CONCLUSIONS

(Al-Si-Cu)-N films were sputter-reactive deposited on silicon substrates, at different conditions. The FTIR investigations in (Al-Si-Cu)-N films, show that Al-N bonds are strengthened by the increasing of nitrogen flow. Similar results are founded by the increasing the deposition power.

Furthermore, absorption peaks related to the others bonding of film material were not founded. When nitrogen flow increases, the surface morphology of the films becomes rougher. The nitrogen concentrations hardly affect the refraction index of the films. From the FTIR results and deposition rate it is evident the existence of an inflection point in the deposition rate values defining a range of nitrogen flow to deposit nitride films and another to deposit metallic films. The inflection point occurs at a critical flux 40 sccm of nitrogen reactive gas.

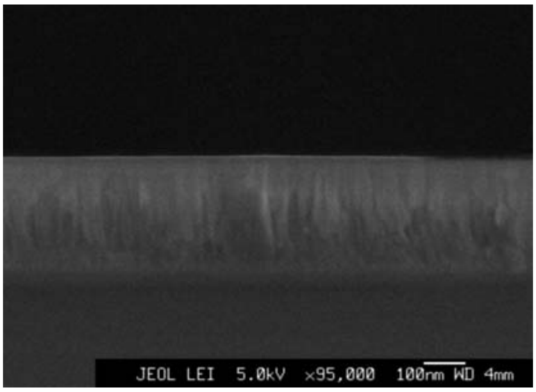

Figure 12 - The surface cross sectional SEM-FEG image of (Al-Si-Cu)-N film, deposited at 4 KW deposition power. Flows were applied at 50 sccm and 75sccm for argon and nitrogen respectively. All films are extremely dense with no discernible structural features or defects.

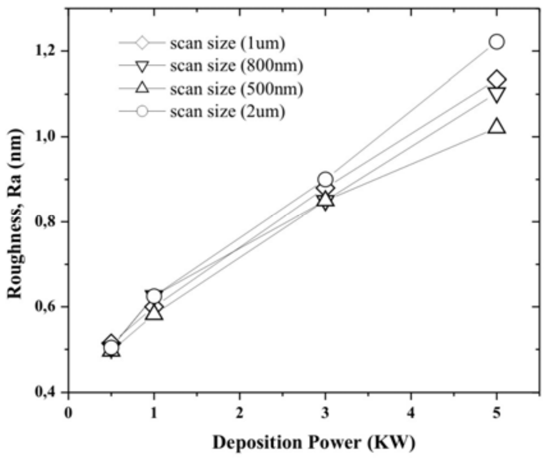

Figure 13 - Roughness versus deposition power. Samples deposited in accordance to series 1.

Since the examination with SEM-FEG did not give any indication that the thin films might be porous, we consider the assumption piezoelectric properties to be valid even for poorly textured (Al-Si-Cu)-N films. Thus, polycrystalline (Al-Si-Cu)-N thin films sputtered on silicon substrates are well suited for the use as actuator layers in micromechanical systems.

ACKNOWLEDGMENTS

The authors would like to thank Mr. Eduardo A. Zambotti, for the technical assistance in the sputtering equipment. This work was supported by CNPq, CAPES and FAPESP. The FE-SEM, SEM/EDS and AFM characterizations of the samples have been performed with equipments of the LME & AFM, both installations of the LNLS.

REFERENCES

1. MORLET, V.; ELMAZRIA, O.; NESLADEK. M;. D´HAEN, J.; VANHOYLAND, G.; ELHAKIKI, M.; TAJAN, A.; BUSTARRET, E.; GHEERAERT, E.; D´OLIESLAEGER,M.; ALNOT, P., *Diamond and Related Materials* 12 (2003) 723.
2. HUANG, CH-L.; TAY, K-W.; WU, L., *Solid-State Electronics* 49 (2005) 219.
3. TAY, K-W.; HUANG, CH-L.; WU, L.; *Journal of the Vacuum Science and Technology B* 23 (2005) 1474.
4. ABRECHT, M.; ARIOSA, D.; ONELLION, M.; MARGARITONDO, G.; PAVUNA, D., *Journal of Applied Physics* 91 (2002) 1187.
5. ELMAZRIA, O.; BÉNÉDIC, F.; EL HAKIKI, M.; MOUBCHIR, H.; ASSOUAR, M.B.; SILVA, F., *Diamond & Related Materials* 15 (2006) 193.
6. WANG, M-C.; TSAI, M-S.; WU, N-C., *Journal of Materials Science* 36 (2001) 3283.
7. BALASUBRAMANIAN, C.; GODBOLE, V.P.; ROHATGI, V.K.; DAS, A.K.; BHORASKAR, S.V., *Nanotechnology* 15 (2004) 370.
8. ASSOUAR, M.B.; ELMAZRIA, O.; ELHAKIKI, M.; ALNOT, P., *Journal of the Vacuum Science and Technology* B 22 (2004) 1717.
9. MORTET, V.; VASIN, A.; JOUAN, P.Y.; ELMAZRIA, O.; DJOUADI, M.A., *Surface and Coatings Technology* 176 (2003) 88.
10. MARTIN, F.; JAN, M.E.; BELGACEM, B.; DUBOIS, M.A.; MURALT, P., *Thin Solid Films* 514 (2006) 341.
11. SMENTKOWSKI, V.S., *Progress in Surface Science* 64 (2000) 1.
12. YING, F.; SMITH, R.W.; SROLOVITZ, D.J., *Applied Physics Letters* 69 (1996) 307.
13. KELLER, J.H.; SIMONS, R.G., *IBM Journal of Research and Development* 23 (1979) 24.
14. ZHANG, J.X.; CHENG, H.; CHEN, Y.Z.; UDDIN, A.; YUAN, S.; GENG, S.J.; ZHANG, S., *Surface & Coatings Technology* 198 (2005) 68.
15. SANZ-HERVA´S, A.; IBORRA, E.; CLEMENT, M.; SANGRADOR, J.; AGUILAR, M., *Diamond and Related Materials* 12 (2003) 1186.
16. YOU, Y.Z.; KIM, D., *Thin Solid Films* 515 (2007) 2860.
17. ZOU, W.; WADLEY, H.N.G.; ZHOU, X.W.; GHOSAL, S.; KOSUT, R.; BROWNELL, D., *Journal of the Vacuum Science and Technology A* 19 (2001) 2414.